EasyChair Preprint

№ 693

Simulation research of impact of number of coils in EMT sensors on reconstructed images quality

Xianglong Liu, Ze Liu and Yuanli Yue

December 23, 2018

Simulation research of impact of number of coils in EMT sensors on reconstructed images quality

Xianglong Liu, Ze Liu and Yuanli Yue

School of Electronic and Information Engineering, Beijing Jiaotong University, Beijing, 100044, China
Corresponding author email: zliu@bjtu.edu.cn

Abstract Electromagnetic tomography (EMT) has been developed for visualizing the conductivity distribution of materials with multi-coil electromagnetic sensors. It is crucial to design an EMT sensor for the improvement of reconstructed images quality. The selection of the number of coils is discussed in this paper due to its great importance to system performance and system complexity. It is commonly believed that more coils in EMT sensor would obtain better performance of reconstructed images. In order to study the impact of number of coils in EMT sensors on quality of reconstructed images, five kinds of sensors with different number of coils including 4, 8, 12, 16 and 20, are involved to conduct numerical simulations. EMT forward problem can be solved through implementing finite element method (FEM), then measurements and sensitivity matrix are obtained, which can be used to solve EMT inverse problem with proper image reconstruction algorithms. Five typical conductivity distributions are used to verify the performance of EMT sensors with different number of coils. The sensitivity matrices of different EMT sensors are analyzed to further explain the essential reason of these numerical simulation results using singular value decomposition (SVD). It can be concluded that EMT sensor with 16 coils produces the best image reconstruction results for most of the typical conductivity distributions. Limited improvement can be obtained in the quality of reconstructed images when the number of coils is more than 16.

Keywords electromagnetic tomography, image reconstruction, conjugate gradient, Landweber iteration, inverse problem, singular value decomposition (SVD), sensitivity matrix.

1 Introduction

Electromagnetic tomography is an emerging measurement technique for visualizing cross-sectional images of electrically conductive or magnetically permeable materials based on the induced voltages obtained from the detection coils evenly distributed around the vessels and pipelines [1-2]. EMT has several advantages over other process tomography techniques such as non-invasive, non-contact, low

cost, high speed, small size and easy to use, so it has great potential and can be used to both industrial and biomedical applications such as multiphase flow measurement [3-4], visualization of molten metal [5-6], nondestructive testing [7], brain oedema detection [8], et al. EMT has been extensively developed over the past two decades including hardware design, image reconstruction algorithms and potential applications. As for EMT sensors, the commonly used sensor geometry is circular shape with 8 coils around the periphery of the sensor. However, there is limited improvement for EMT sensors.

There is great potential to improve the performance of EMT technique through intense research into EMT sensors. Most of the EMT sensors are circular, namely O-shaped sensors. Circular EMT sensors can be used to vessels and pipelines for multiphase flow measurement. However, some other kinds of EMT sensors are developed to adapt specific measurement conditions. Ma *et al*. [9] studied the C-shaped EMT sensor which is easy to be removed rapidly and assessed its performance for steel flow visualization. They concluded that the EMT system will be more ill posed with the number of coils in EMT sensors further reduced. Yin and Peyton [10] developed a planar inductive sensors with axes of all the coils perpendicular to the object space, which is used for nondestructive testing to a metallic disc. Liu *et al*. [7] proposed a new L-shaped EMT sensor used to conduct rail defect inspection. Simulations and laboratory experiment results verified the feasibility of the EMT method with L-shaped sensor. Ma and Soleimani [11] addressed the issue of hidden defect identification in carbon fibre reinforced polymer (CFRP) using a dual plane EMT sensor array.

Peng *et al*. [12] studied the effect of number of electrodes in ECT sensors on image quality and proved that limited improvement can be obtained through simply increasing the number of electrodes. Finally, they recommended that 12-electrode sensor can be used for most applications. Ye *et al*. [13] discussed the effect of the number of electrodes in ERT sensor on image quality and drew a conclusion that different number of pixels in the sensing domain required different number of electrodes to obtain the best images for most distributions. However, there is hardly any report on the impact of number of coils in EMT sensors on reconstructed images quality.

In this paper, the impact of number of coils in EMT sensors on the quality of reconstructed images is systematically discussed. It is commonly assumed that more coils result in more independent measurements, thus obtaining better quality of reconstructed images. However, EMT sensor with more coils will lead to high requirement for hardware. In order to better determine the proper number of coils for EMT sensors, numerical simulations of EMT sensors with different number of coils including 4, 8, 12, 16 and 20, are implemented in this paper. Finally, image reconstructions are conducted with three typical image reconstruction algorithms including Tikhonov regularization method, projected Landweber iteration algorithm [14-15] and conjugate gradient algorithm [16] for five typical conductivity distributions to study the proper number of coils for EMT sensors.

2 Theory

2.1 Principle of EMT and structure of EMT sensor

EMT is based on electromagnetic induction principles, which is composed of EMT sensor array, conditioning electronics and a host computer. Several coils are evenly distributed around the periphery of imaging region. When alternating current is injected into the excitation coil, alternating magnetic field is generated within the whole imaging region. The secondary magnetic field is generated due to the eddy current induced in the test conductive objects, which couples with the primary magnetic field and makes the primary field distorted. The induced voltages are measured from the detection coils. The commonly used measurement strategy for EMT is single coil excitation. One of the coils is selected as the excitation coil, the rest of the coils are chosen as the detection coils. The process continues until each of the coils is selected as the excitation coil. All the induced voltages between arbitrary two coils combination are obtained. Image reconstruction can be conducted with the measurements and sensitivity matrix using iterative or non-iterative image reconstruction algorithms.

EMT sensor is the most important part for the performance of EMT system. O-shaped sensor is the widely used structure for EMT sensor. The impact of number of coils in EMT sensors on quality of reconstructed images is discussed in this paper. Fig. 1 shows the five kinds of EMT sensors with different number of coils.

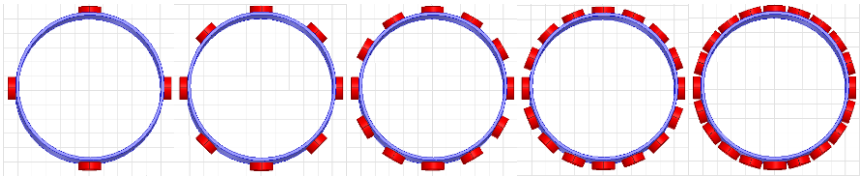

(a) 4-coil. (b) 8-coil. (c) 12-coil. (d) 16-coil. (e) 20-coil

Fig. 1 Five kinds of EMT sensors with different number of coils

2.2 EMT inverse problem

The most important step for EMT inverse problem is image reconstruction, which is to generate cross-sectional images from the measurements and sensitivity matrix. The relationship between the induced voltages and the conductivity distribution inside the imaging region is described as follows

$$V_{ij} = \iint_C \sigma(x,y) F\left(x,y,\sigma(x,y)\right) \mathrm{d}x\mathrm{d}y \tag{1}$$

where V_{ij} is the induced voltage between coil pair *i-j*, σ is the conductivity distribution, F is the sensing field distribution function and C is the cross-sectional area of the imaging region.

Due to the fact that solving equation (1) is too complicated, linear approximation method is implemented through assuming that the sensing field function has nothing to do with the conductivity distribution inside the imaging region. After discretization, linearization and normalization, the linear equation between the induced voltage and conductivity distribution is shown as follows

$$U = Sg \tag{2}$$

where $\boldsymbol{U}$ is the normalized measurement voltage vector, $\boldsymbol{S}$ is the normalized sensitivity matrix and $\boldsymbol{g}$ is the normalized conductivity distribution vector.

To solve EMT inverse problem, the sensitivity matrix is obtained as the prior information in the stage of solving the EMT forward problem. Sensitivity matrix reflects the refined change of induced voltage due to the change of conductivity distribution inside imaging region. The relationship is expressed as follows [11]

$$\frac{\partial V_{ij}}{\partial \sigma_k} = -\omega^2 \frac{\int_{\Omega_k} A_i \cdot A_j d\upsilon}{I_i I_j} \tag{3}$$

where V_{ij} is the induced voltage between coil pair *i-j*, σ_k is the conductivity distribution of element k and ω is angular frequency. $\boldsymbol{A}_i$ and $\boldsymbol{A}_j$ are forward problem solvers when coils i and j are excited by I_i and I_j, respectively. Ω_k is the volume of perturbation (element k). Sensitivity matrix can be obtained by perturbation method including simulation perturbation method and experiment perturbation method, and semi-analysis method.

The essence of EMT inverse problem is actually to determine the conductivity distribution based on equation (2). Due to the absence of inverse matrix of sensitivity matrix, there is no analytical solution to equation (2). EMT inverse problem is ill-posed and ill-conditioned due to the soft field characteristic of electromagnetic sensing field, so it is always transformed into optimization problem. Optimization methods can be applied to solve EMT inverse problem. In this paper, Tikhonov regularization method, projected Landweber iteration algorithm and conjugate gradient algorithm are used to reconstruct the five kinds of typical conductivity distributions. Tikhonov regularization is the most widely used regularization method, which is expressed as follows

$$g = \left(S^{\mathrm{T}} S + \mu \mathrm{I}\right)^{-1} S^{\mathrm{T}} U \tag{4}$$

where $\boldsymbol{S}^{\mathrm{T}}$ is the transpose of normalized sensitivity matrix $\boldsymbol{S}$, μ denotes the regularization parameter.

Besides Tikhonov regularization method, iterative algorithms are also used to solve equation (2). The projected Landweber iteration is the commonly used iterative algorithm, which is expressed as follows:

$$g_{k+1} = P\left[g_k - \alpha S^{\mathrm{T}}\left(Sg_k - U\right)\right] \tag{5}$$

where k is the iteration number, α is the relaxation factor and P is the projection operator which is described as

$$P\left[f(g)\right] = \begin{cases} 0 & \text{if } f(g) < 0 \\ f(g) & \text{if } 0 \le f(g) \le 1 \\ 1 & \text{if } f(g) > 1 \end{cases} \tag{6}$$

Conjugate gradient (CG) algorithm is an effective global iterative method for its iteration simplicity and low memory requirements. It requires the coefficient matrix to be symmetric and positive definite. In order to use CG algorithm, equation (2) is transformed into equation (7) by multiplying both sides by $\boldsymbol{S}^{\mathrm{T}}$.

$$b = Ag \tag{7}$$

where $b = S^{\mathrm{T}}U$, $A = S^{\mathrm{T}}S$.

The iterative scheme of conjugate gradient algorithm is shown as follows

$$\begin{cases} g_0 = \left(S^{\mathrm{T}}S + \mu \mathrm{I}\right)^{-1} S^{\mathrm{T}}U \\ g_{k+1} = g_k + \lambda_k p_k \end{cases} \tag{8}$$

where g_0 is the initial value obtained by Tikhonov regularization method, λ_k is the step factor, and p_k is the search direction. λ_k and p_k are defined as follows

$$\lambda_k = \frac{r_k^{\mathrm{T}} r_k}{p_k^{\mathrm{T}} A p_k} \tag{9}$$

$$p_k = \begin{cases} r_k & k = 0 \\ r_k + \beta_k p_{k-1} & k > 0 \end{cases} \tag{10}$$

where r_k is the residual vector and it is expressed as follows:

$$r_k = \begin{cases} b - Ag_0 & k = 0 \\ r_{k-1} - \lambda_{k-1} A p_{k-1} & k > 0 \end{cases} \tag{11}$$

Besides, β_k is obtained using Fletcher-Reeves (FR) method, which is defined as follows

$$\beta_k = \frac{\|r_k\|^2}{\|r_{k-1}\|^2} \tag{12}$$

The iteration procedure stops when the maximum number of iterations is satisfied.

3. Numerical simulation

In order to study the impact of different number of coils in EMT sensors on the quality of reconstructed images. Electromagnetic sensors with different number of coils including 4, 8, 12, 16 and 20 are involved to reconstruct the five kinds of typical conductivity distributions with Tikhonov regularization method, projected Landweber iteration algorithm and conjugate gradient algorithm, respectively. Fig. 2 shows the five kinds of typical conductivity distributions inside the imaging region. EMT forward problem is solved by finite element method. The computation of EMT forward problem is running on an environment with commercial software. The excitation strategy is single coil excitation. The whole measurement procedure is controlled by VBA script function embedded in Excel, which can automatically invoke the commercial software to complete the computation of EMT forward problem. EMT inverse problem is solved by Matlab using Tikhonov regularization method, projected Landweber iteration algorithm and conjugate gradient algorithm for EMT sensors with different number of coils.

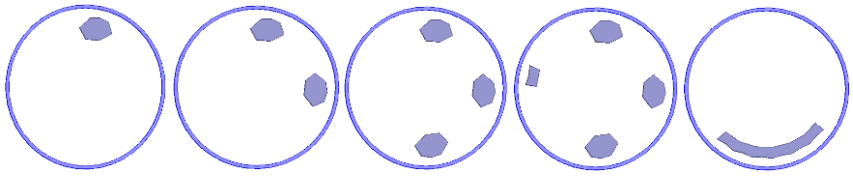

Fig. 2 Five kinds of typical conductivity distributions

3.1. With Tikhonov regularization method

Table 1 shows the reconstructed images using EMT sensors with different number of coils for five typical conductivity distributions with Tikhonov regularization method. Tables 2 and 3 show the correlation coefficients and image errors between the reconstructed images and true conductivity distributions.

Table 1 Reconstructed images by Tikhonov regularization method

Coils	Distribution 1	Distribution 2	Distribution 3	Distribution 4	Distribution 5
4	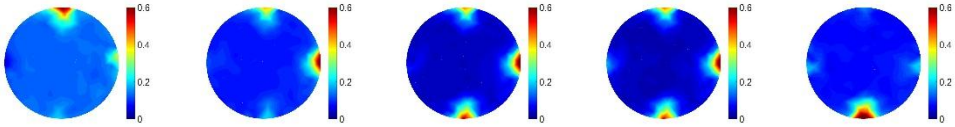				
8	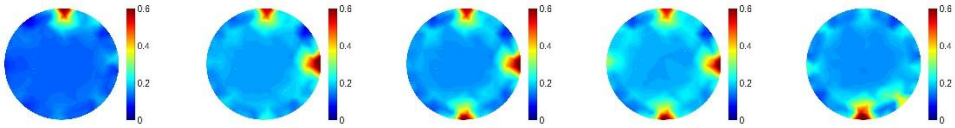				
12	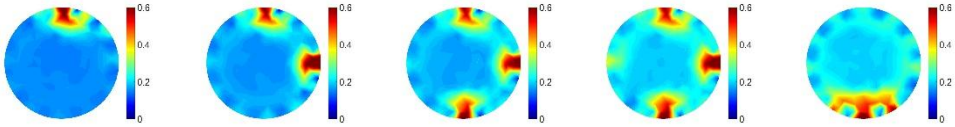				
16	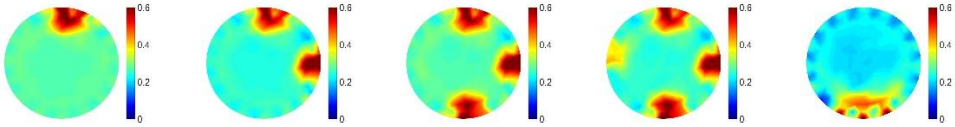				
20	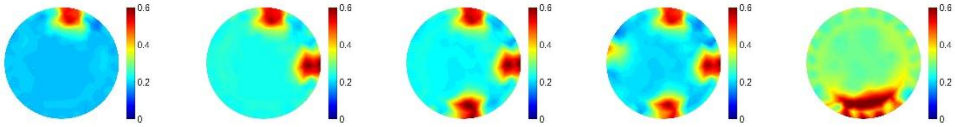				

Table 2 Correlation coefficients

Coils	Distribution 1	Distribution 2	Distribution 3	Distribution 4	Distribution 5
4	0.2327	0.2184	0.2846	0.2580	0.1649
8	0.3402	0.3697	0.3507	0.3179	0.2038
12	0.4894	0.5437	0.5295	0.4954	0.3008
16	0.5172	0.5640	0.5522	0.5172	0.2563
20	0.6113	0.6339	0.6425	0.5813	0.3519

Table 3 Image errors

Coils	Distribution 1	Distribution 2	Distribution 3	Distribution 4	Distribution 5
4	0.6452	0.5107	0.4735	0.4736	0.4999
8	0.6221	0.5813	0.5210	0.5191	0.5555
12	0.6820	0.5651	0.5182	0.5287	0.6077
16	1.0087	0.7023	0.6458	0.5999	0.6174
20	0.7261	0.6517	0.5483	0.5137	0.7390

As shown in Tables 1, 2 and 3, EMT sensor with 4 coils gives the worst reconstructed images for all the five typical conductivity distributions due to lack of independent measurements. The quality of reconstructed images becomes better with the increase of the number of coils in terms of the five typical conductivity distributions. EMT sensor with 20 coils obtains the largest correlation coefficients between the reconstructed images and true conductivity distributions. EMT sensor with 16 coils obtains the correlation coefficients only second to EMT sensor with 20 coils. In general, the quality of reconstructed images is slightly improved with the number of coils increasing from 12 to 20 coils in terms of the correlation coefficients.

3.2. With projected Landweber iteration algorithm

Table 4 shows the reconstructed images using EMT sensors with different number of coils for the five typical conductivity distributions with projected Landweber iteration algorithm. Tables 5 and 6 show the correlation coefficients and image errors between the reconstructed images and true conductivity distributions.

Table 4 Reconstructed images by projected Landweber iteration algorithm

Coils	Distribution 1	Distribution 2	Distribution 3	Distribution 4	Distribution 5
4	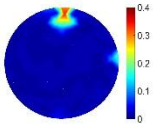	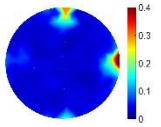	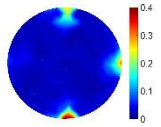	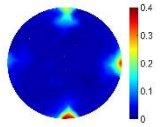	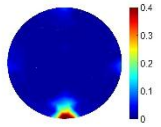
8	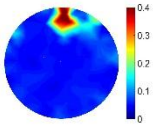	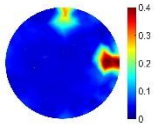	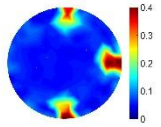	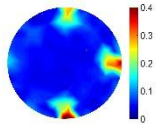	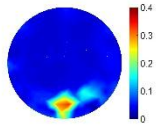
12	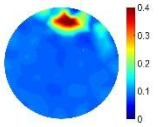	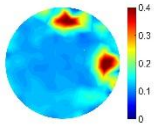	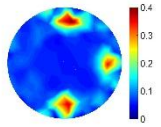	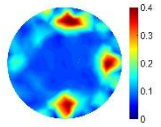	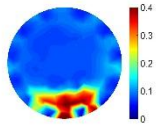
16	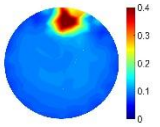	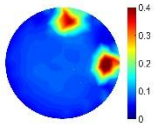	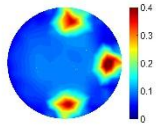	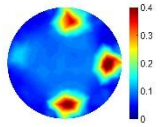	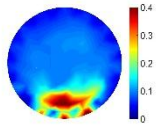
20	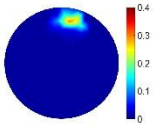	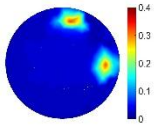	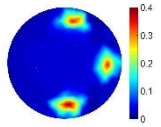	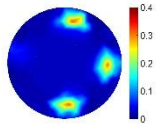	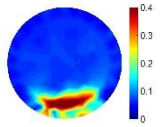

Table 5 Correlation coefficients

Coils	Distribution 1	Distribution 2	Distribution 3	Distribution 4	Distribution 5
4	0.3904	0.2508	0.2023	0.1740	0.0870
8	0.5266	0.5413	0.4769	0.3975	0.2144
12	0.6900	0.7089	0.6675	0.6200	0.2626
16	0.6796	0.7384	0.7415	0.6939	0.2267
20	0.6523	0.7175	0.7330	0.6680	0.3475

Table 6 Image errors

Coils	Distribution 1	Distribution 2	Distribution 3	Distribution 4	Distribution 5
4	0.4605	0.4814	0.4805	0.4840	0.5015
8	0.4562	0.4132	0.4271	0.4412	0.4781
12	0.4517	0.4285	0.3801	0.3932	0.4987
16	0.4658	0.3653	0.3614	0.3692	0.5013
20	0.3895	0.3721	0.3570	0.3888	0.4729

It can be seen from Tables 4, 5 and 6, 4-coil EMT sensor suffers from severe non-linear distortion, particularly for distributions 4 and 5. For distribution 1, 12-coil EMT sensor can obtain the best images. For distributions 2, 3 and 4, 16-coil EMT sensor gives the best images in terms of the correlation coefficients. For distribution 5, the quality of reconstructed images obtained by 20-coil EMT sensor is better than that of other sensors. In general, the quality of reconstructed images is improved with the number of coils increasing from 4 coils to 16 coils in terms of the correlation coefficients. Therefore, 16-coil EMT sensor is recommended as the first choice for EMT system when considering both system performance and system complexity.

3.3. With conjugate gradient algorithm

Table 7 shows the reconstructed images using EMT sensors with different number of coils for the five typical conductivity distributions with conjugate gradient algorithm. Tables 8 and 9 show the correlation coefficients and image errors between the reconstructed images and true conductivity distributions, respectively.

As can be seen from Tables 7, 8 and 9, 4-coil EMT sensor obtains the worst results due to few measurements than the number of elements, especially for multiple objects such as distributions 4 and 5. For distributions 1, 2, 3 and 4, 16-coil EMT sensor gives the best images. For distribution 5, 20-coil EMT sensor obtains the best images. In general, the quality of reconstructed images is greatly

Table 7 Reconstructed images by conjugate gradient algorithm

Coils	Distribution 1	Distribution 2	Distribution 3	Distribution 4	Distribution 5
4	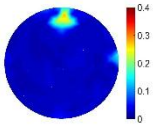	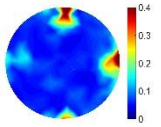	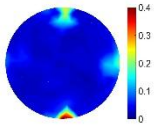	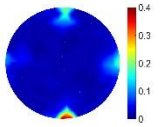	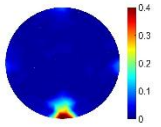
8	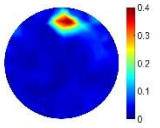	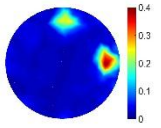	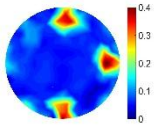	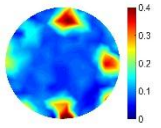	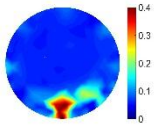
12	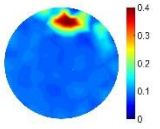	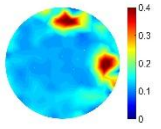	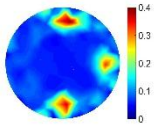	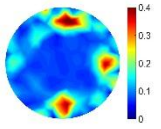	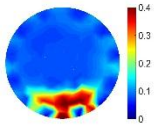
16	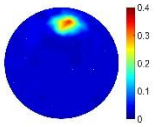	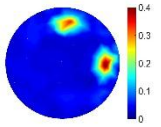	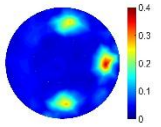	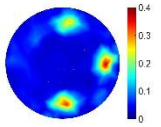	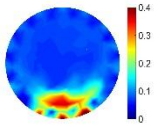
20	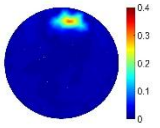	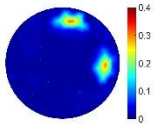	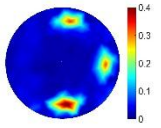	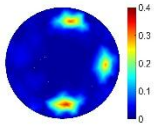	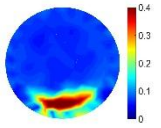

Table 8 Correlation coefficients

Coils	Distribution 1	Distribution 2	Distribution 3	Distribution 4	Distribution 5
4	0.4575	0.3438	0.2356	0.1638	0.1074
8	0.6631	0.6738	0.5911	0.4756	0.2501
12	0.6863	0.6875	0.6537	0.5905	0.2683
16	0.7020	0.7280	0.7080	0.6632	0.2034
20	0.6451	0.6858	0.6965	0.6354	0.3610

Table 9 Image errors

Coils	Distribution 1	Distribution 2	Distribution 3	Distribution 4	Distribution 5
4	0.4406	0.4843	0.4732	0.4845	0.4997
8	0.3781	0.3782	0.3957	0.4303	0.4801
12	0.4558	0.4393	0.3842	0.4008	0.4982
16	0.3776	0.3577	0.3782	0.3858	0.5018
20	0.3874	0.3787	0.3627	0.3924	0.4669

improved with the number of coils increasing from 4 to 8 and slightly improved with the number of coils increasing from 8 to 16.

3.4. Analysis of sensitivity matrices

Table 10 Sensitivity distributions of two coil pairs for EMT sensors with different number of coils

Coil pairs	4	8	12	16	20
adjacent	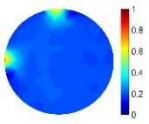	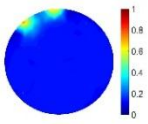	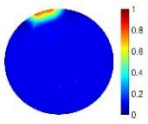	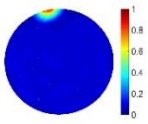	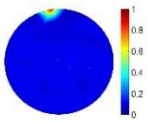
opposite	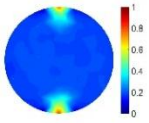	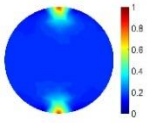	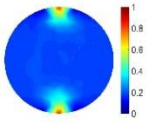	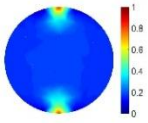	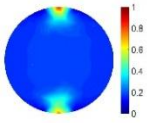

Table 10 shows sensitivity distributions of two coil pairs for EMT sensors with different number of coils. It can be seen from Table 10 that the sensitivity distributions is approximately the same when the number of coils is more than 16, which means the EMT sensors are apt to possess the same properties.

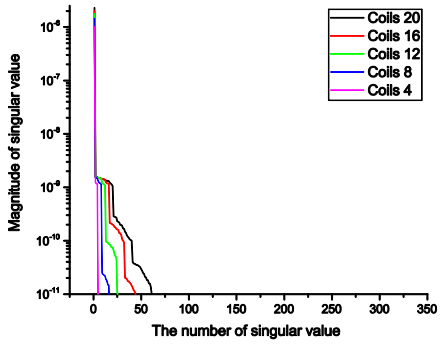

Fig. 3 Singular values spectrum

Singular values spectrum of sensitivity matrices for EMT sensors with different number of coils including 4, 8, 12, 16 and 20 are obtained, which are plotted in Fig. 3. It can be seen from Fig. 3 that most of the singular values tend to be zero

when the number of coils is more than 16, which means the sensitivity matrix becomes more singular.

4. Conclusion

The impact of different number of coils in EMT sensors on the quality of reconstructed images are studied in this paper. Five kinds of EMT sensors with different number of coils including 4, 8, 12, 16 and 20 are involved to conducted EMT forward problem computations. Three commonly used image reconstruction algorithms are applied to obtain the reconstructed images for EMT sensors. Five typical conductivity distributions are used to verify the performance of EMT sensors with different number of coils. Numerical simulation results show that EMT sensor with 16 coils gives the best image reconstruction results for most of the conductivity distributions. Limited improvement can be obtained in the quality of reconstructed images when the number of coils is more than 16. In general, 16-coil EMT sensor is recommended as the first choice for most applications when considering the quality of reconstructed images and system complexity.

Acknowledgments

This work was supported by the National Natural Science Foundation of China under Grant 61771041.

REFERENCES

[1] Peyton, A. J., et al. (1996). An overview of electromagnetic inductance tomography: description of three different systems. *Measurement Science and Technology*, *7*, 261-271.

[2] Ma, L., & Soleimani, M. (2017). Magnetic induction tomography methods and applications: a review. *Measurement Science and Technology*, *28*, 1-12.

[3] Liu, Z., Yang, G. Y., He, N., & Tan, X. Y. (2012). Landweber iterative algorithm based on regularization in electromagnetic tomography for multiphase flow measurement. *Flow Measurement and Instrumentation*, *27*, 53-8.

[4] Terzija, N., Yin, W., Gerbeth, G., et al. (2011). Use of electromagnetic induction tomography for monitoring liquid metal/gas flow regimes on a model of an industrial steel caster. *Measurement Science and Technology*, *22*, 1-8.

[5] Binns, R., Alyons, A. R., & Peyton, A. J. (2001). Imaging molten steel flow profiles. *Measurement Science and Technology*, *12*, 1132-1138.

[6] Ma, X. D., Peyton, A. J., Binns, R., & Higson, S. R. (2005). Electromagnetic techniques for imaging the cross-section distribution of molten steel flow in the continuous casting nozzle. *IEEE Sensors Journal*, *5*, 224-232.

[7] Liu, Z., Li, W., Xue, F., Xiafang, J., Bu, B., & Yi, Z. (2015). Electromagnetic tomography rail defect inspection. *IEEE Transactions on Magnetics*, *51*, 1-7.

[8] Merwa, R., Hollaus, K., Oszkar, B., & Scharfetter, H. (2004). Detection of brain oedema using magnetic induction tomography: a feasibility study of the likely sensitivity and detectability. *Physiological Measurement*, *25*, 347-354.

[9] Ma, X., Peyton, A. J., Higson, S. R., & Drake, P. (2008). Development of multiple frequency electromagnetic induction systems for steel flow visualization. *Measurement Science and Technology*, *19*, 094008.

[10] Yin, W., & Peyton, A. J. (2006). A planar EMT system for the detection of faults on thin metallic plates. *Measurement Science and Technology*, *17*, 2130-2135.

[11] Ma, L., & Soleimani, M. (2014). Hidden defect identification in carbon fibre reinforced polymer plates using magnetic induction tomography. *Measurement Science and Technology*, *25*, 055404.

[12] Peng, L. H., Ye, J. M., Lu, G., & Yang, W. Q. (2012). Evaluation of effect of number of electrodes in ECT sensors on image quality. *IEEE Sensors Journal*, *12*, 1554-1565.

[13] Ye, J. M., Wang, H. G., & Yang, W. Q. (2013). Evaluation of effect of number of electrodes in ERT sensors on image quality. *2013 IEEE International Conference on Imaging Systems and Techniques (IST)*, 19-24.

[14] Yang, W. Q., Spink, D. M., York, T. A., & Mccann, H. (1999). An image-reconstruction algorithm based on Landweber's iteration method for electrical-capacitance tomography. *Measurement Science and Technology*, *10*, 1065-1069.

[15] Yang, W. Q., & Peng, L. H. (2003). Image reconstruction algorithms for electrical capacitance tomography. *Measurement Science and Technology*, *14*, 1-13.

[16] Wang, M. (2002). Inverse solutions for electrical impedance tomography based on conjugate gradients methods *Measurement Science and Technology*, *13*, 101-117.